RESEARCH ARTICLE

*Journal of* Cellular Physiology WILEY

# Functional differences in agonist-induced plasma membrane expression of Orai1α and Orai1β

Isaac Jardin [ID] | Sandra Alvarado | Jose Sanchez-Collado [ID] | Joel Nieto-Felipe [ID] |
Jose J. Lopez [ID] | Gines M. Salido [ID] | Juan A. Rosado [ID]

Department of Physiology (Cellular Physiology Research Group), Institute of Molecular Pathology Biomarkers (IMPB), University of Extremadura, Caceres, Spain

**Correspondence**
Isaac Jardin and Juan A. Rosado, Department of Physiology (Cellular Physiology Research Group), Institute of Molecular Pathology Biomarkers (IMPB), University of Extremadura, 10003 Caceres, Spain.
Email: ijp@unex.es and jarosado@unex.es

## Abstract

Orai1 is the pore-forming subunit of the store-operated $Ca^{2+}$ release-activated $Ca^{2+}$ (CRAC) channels involved in a variety of cellular functions. Two Orai1 variants have been identified, the long form, Orai1α, containing 301 amino acids, and the short form, Orai1β, which arises from alternative translation initiation from methionines 64 or 71, in Orai1α. Orai1 is mostly expressed in the plasma membrane, but a subset of Orai1 is located in intracellular compartments. Here we show that $Ca^{2+}$ store depletion leads to trafficking and insertion of compartmentalized Orai1α in the plasma membrane via a mechanism that is independent on changes in cytosolic free-$Ca^{2+}$ concentration, as demonstrated by cell loading with the fast intracellular $Ca^{2+}$ chelator dimethyl BAPTA in the absence of extracellular $Ca^{2+}$. Interestingly, thapsigargin (TG) was found to be unable to induce translocation of Orai1β to the plasma membrane when expressed individually; by contrast, when Orai1β is co-expressed with Orai1α, cell treatment with TG induced rapid trafficking and insertion of compartmentalized Orai1β in the plasma membrane. Translocation of Orai1 forms to the plasma membrane was found to require the integrity of the actin cytoskeleton. Finally, expression of a dominant negative mutant of the small GTPase ARF6, and ARF6-T27N, abolished the translocation of compartmentalized Orai1 variants to the plasma membrane upon store depletion. These findings provide new insights into the mechanism that regulate the plasma membrane abundance of Orai1 variants after $Ca^{2+}$ store depletion.

**KEYWORDS**
actin cytoskeleton, ARF6, Orai1α, Orai1β, plasma membrane, store-operated $Ca^{2+}$ entry

## 1 | INTRODUCTION

Store-operated $Ca^{2+}$ entry (SOCE) is a major mechanism for $Ca^{2+}$ influx that plays a relevant functional role in a variety of cellular processes from the maintenance of intracellular $Ca^{2+}$ homeostasis and signals to gene transcription. The key molecular elements of the store-operated channels are the endoplasmic reticulum (ER) $Ca^{2+}$ sensors of the STIM family and the $Ca^{2+}$ permeable channels of the Orai family (Ahmad et al., 2022; Emrich et al., 2022). Agonist-induced discharge of the intracellular $Ca^{2+}$ stores results in a conformational

change of the STIM proteins, which, in turn, leads to store-dependent activation of Orai channels in the plasma membrane (Lunz et al., 2019; Yen & Lewis, 2019; Zhou et al., 2017). Orai1 and its mammalian paralogs, Orai2 and Orai3, have been suggested to hetero-multimerize to match the extent of $Ca^{2+}$ influx to the strength of agonist stimulation (Emrich et al., 2021; Yoast et al., 2020).

Orai1 recycles dynamically and rapidly at the plasma membrane (Hodeify et al., 2015). The chaperonin-containing T-complex protein 1 (CCT) has been reported to modulate Orai1 recycling by modulating Orai1 endocytosis (Hodeify et al., 2018). $Ca^{2+}$ store depletion leads to the accumulation of Orai1 in the plasma membrane by a mechanism that requires the participation of proteins of the exocytotic machinery, such as the synaptosomal-associated protein-25 (SNAP-25) (Woodard et al., 2008). The accumulation of Orai1 in the plasma membrane upon store depletion is then facilitated by a STIM1-dependent Orai1 "trafficking trap" mechanism that retains Orai1 in the cell surface, reducing the recycling or compartmentalized pool (Hodeify et al., 2015).

Two Orai1 variants have been identified in mammalian cells, the long form, Orai1α, which contains 301 amino acids, and the short variant, Orai1β, which arises from the same transcript by alternative translation initiation from a methionine at position 64, and perhaps 71, in the long form (Fukushima et al., 2012). Despite both variants supporting the store-operated and highly $Ca^{2+}$ selective current $I_{CRAC}$ with similar efficacy (Desai et al., 2015), several functional and biophysical differences between the two variants have been shown. Concerning the functional differences, in addition to $I_{CRAC}$, Orai1α participates in the less $Ca^{2+}$ selective store-operated current $I_{SOC}$, which involves the participation of STIM1 and the transient receptor potential channel family member TRPC1 (Cheng et al., 2011; Jardin et al., 2008; Kim et al., 2009), as well as in the arachidonate-regulated current, $I_{ARC}$ (Desai et al., 2015). By contrast, Orai1β does not support $I_{ARC}$, and its participation in $I_{SOC}$ is cell specific (Sanchez-Collado et al., 2022). Moreover, Orai1α but not Orai1β is required for the activation of the transcription factor NF-κB (Nieto-Felipe et al., 2023). Some differences in the biophysical properties have also been reported, including that Orai1α is more sensitive to fast $Ca^{2+}$-dependent inactivation than Orai1β (Desai et al., 2015). Here we report significant differences in the efficacy of Orai1α and Orai1β to accumulate at the plasma membrane following store depletion. While $Ca^{2+}$ store depletion induces plasma membrane enrichment of Orai1α when expressed either singly or together with Orai1β, the latter behaves as a defective protein that requires the presence of Orai1α to accumulate in the plasma membrane after store depletion.

## 2 | MATERIAL AND METHODS

### 2.1 | Cell culture and transfections

CRISPR-generated Orai1 single-knockout HEK293 cells (O1KO) and parental HEK-293 cells were kindly provided by Mohamed Trebak and cultured at 37°C with a 5% $CO_2$ in high-glucose Dulbecco's modified Eagle's medium (DMEM; 15323531; ThermoFisher Scientific) supplemented with 10% (v/v) fetal bovine serum (11573397; ThermoFisher Scientific) and 100 U/mL penicillin and streptomycin (11548876; ThermoFisher Scientific), as described previously (Nieto-Felipe et al., 2023). For transient transfections, cells were grown to 60%–80% confluency and transfected with TK-promoter Orai1α-eGFP or Orai1β-eGFP or CMV-promoter Orai1α-eGFP or Orai1β-eGFP, depending on the experimental conditions, using DharmaFECT kb transfection reagent (77T-2006-01, Dharmacon) and were used 48 h after transfection. For western blot analysis and biotinylation, cells ($5 \times 10^6$) were plated in 100-mm petri dish and cultured for 48 h, while, for $Ca^{2+}$ imaging and confocal analysis cells ($4 \times 10^5$) were seeded in a 35-mm six-well multidish. In some experiments, cells were loaded with dimethyl BAPTA by incubation for 30 min with 10 μM dimethyl BAPTA/AM (A1076; Sigma-Aldrich).

### 2.2 | Determination of cytosolic free-$Ca^{2+}$ concentration ($[Ca^{2+}]_c$)

Cells were loaded with fura-2 by incubation with 2 μM fura-2/AM (10308392; ThermoFisher Scientific) for 30 min at 37°C. Coverslips with cultured cells were mounted on a perfusion chamber and placed on the stage of an epifluorescence inverted microscope (Nikon Eclipse Ti2) with an image acquisition and analysis system for videomicroscopy (NIS-Elements Imaging Software v.5.02.00, Nikon). Cells were continuously superfused at room temperature with HEPES-buffered saline (HBS) containing 125 mM NaCl (10428420; ThermoFisher Scientific), 5 mM KCl (P9541; Sigma-Aldrich), 1 mM $MgCl_2$ (141396; Panreac), 5 mM glucose (10141520; ThermoFisher Scientific), and 25 mM HEPES (H3375; Sigma-Aldrich), pH 7.4, supplemented with 0.1% (w/v) BSA (11573397; ThermoFisher Scientific). Cells were examined at 40× magnification (Nikon CFI S FLUOR 40X Oil) and were alternatively excited with light from a xenon lamp passed through a high-speed monochromator Optoscan ELE 450 (Cairn Research) at 340/380 nm. Fluorescence emission at 510 nm was detected using a cooled digital sCMOS camera PCO Panda 4.2 (Excelitas PCO) and recorded using NIS-Elements AR software (Nikon). Fluorescence ratio (F340/F380) was calculated pixel by pixel, and the data were presented as ΔF340/F380. Thapsigargin (TG)-evoked changes in $[Ca^{2+}]_c$ were estimated as the area under the curve measured as the integral of the rise in fura-2 fluorescence 340/380 nm ratio 2.5 min after the addition of the agonist and taking a sample every 2 s.

### 2.3 | Biotinylation protocol

Cells were washed three times with phosphate-buffered saline (PBS, 137 mM NaCl, 2.7 mM KCl, 1.5 mM $KH_2PO_4$, 8 mM $Na_2HPO_4 \bullet 2H_2O$, pH 7.,4), subsequently resuspended in biotinylation buffer (PBS, pH 8.0) and surface labeled with 1 mg/mL sulfo-NHS-LC biotin (21335; ThermoFisher Scientific) at RT. Labeling was stopped 1 h after

reaction with PBS, pH 8.0, supplemented with 100 µM Tris (BP152-1; ThermoFisher Scientific) and washed 2 times in supplemented PBS, pH 8.0. Biotinylated cells were subsequently lysed with ice-cold NP-40 buffer, pH 8.0, containing 137 mM of NaCl, 20 mM of Tris, 2 mM of EDTA, 10% glycerol, 1% Nonidet P-40 (I3032; Sigma-Aldrich), 1 mM of $Na_3VO_4$, and complete EDTA-free protease inhibitor tablets (11836170001; Merk) and protein lysates were incubated with streptavidin-conjugated agarose beads (11886764; Thermo-Fisher Scientific) overnight at 4°C on a rocking platform. Biotinylated proteins bound to streptavidin-conjugated agarose beads were isolated by centrifugation and washed 3 times in NP40 buffer. Biotinylated fraction was loaded and separated in 10% sodium dodecyl sulfate-polyacrylamide gel electrophoresis (SDS-PAGE) and analyzed by western blot analysis using anti-PMCA antibody, as control, or anti-Orai1 (catalog number: O8264, epitope: amino acids 288–301 of human Orai1), as described in Section 2.4. The specificity of the anti-Orai1 antibody was tested in whole-cell lysates from WT HEK-293 cells and O1KO HEK-293 cells (Figure S1). As expected, Orai1 was detected exclusively in WT HEK-293 cells as multiple bands corresponding to the long and short Orai1 variants with different posttranslational modifications, that is, N-linked glycosylation and phosphorylation, among others (Fukushima et al., 2012; Sanchez-Collado et al., 2019).

## 2.4 | Western blot analysis

Western blot analysis was performed as described previously (Sanchez-Collado et al., 2022). Briefly, cells cultured on 100-mm petri dish ($8 \times 10^6$ cells) were stimulated with 2 µM TG or with vehicle and subsequently lysed with ice-cold NP-40 buffer pH 8 containing 137 mM of NaCl, 20 mM of Tris, 2 mM of EDTA, 10% glycerol, 1% Nonidet P-40, 1 mM of $Na_3VO_4$, and complete EDTA-free protease inhibitor tablets. After 20–30 min at 4°C, cell lysates were centrifugated at 10,000 g for 10 min. Next, supernatant was transferred to a fresh tube, the protein concentration was determined by using the BCA Protein Assay kit (23227; ThermoFisher Scientific), and subsequently, equal volume 2X Laemmli sample buffer was added. Cell lysates were resolved by 10% or 12% SDS-PAGE, and separated proteins were electrophoretically transferred onto nitrocellulose membranes for subsequent probing. Blots were incubated overnight with 10% (w/v) BSA in Tris-buffered saline with 0.1% Tween-20 (TBST) to block residual protein binding sites. Immunodetection of Orai1 and PMCA was achieved by incubation for 1 h with anti-Orai1 antibody diluted 1:1000 in TBST and overnight with anti-PMCA antibody diluted 1:500 in TBST. The primary antibody was removed, and blots were washed six times for 5 min each with TBST. To detect the primary antibody, blots were incubated for 1 h with horseradish peroxidase-conjugated goat anti-mouse IgG antibody (115-035-003; Jackson), horseradish peroxidase-conjugated goat anti-rabbit IgG antibody (111-035-003; Jackson) diluted 1:10000 in TBST and then, exposed to enhanced chemiluminiscence reagents for 5 min. The

antibody binding was assessed with a ChemiDoc Imaging System (Bio-Rad) and the density of bands was measured using ImageJ software v.1.8.0_172 (NIH). Data were normalized to the amount PMCA from the same gel.

## 2.5 | Fluorescence recovery after photobleaching (FRAP)

FRAP measurements were carried out on an LSM900 confocal microscope (Carl Zeiss) using a Plan-Apochromat $63 \times 1.4$ Oil objective at a zoom of 1.3X. eGFP was excited with the 488 nm line of 10 mW Diode laser at 1%–4% power to minimalize the bleaching of the sample during monitoring. Fluorescence emission was detected between 492 and 602 nm by an Airyscan detector. The pinhole was set at 1 Airy Unit (23.5099 pixels per micron resolution), and no line averaging was used. The detection gain 700 V was chosen such that the Orai1-eGFP pool at the plasma membrane was almost saturating the dynamic level of the detectors. The FRAP bleaching regions were randomly selected from areas with fluorescence in the dynamic range of the detector. Bleaching area (ROI) was 2.6 µm wide square and not more than 5% of the whole plasma membrane of the targeted cell. Ten bleach iterations, 0.5 s of bleaching time, at 100% transmission of a 10 mW 488 nm laser were sufficient to bleach 80%–90% of eGFP. Three pre-bleach images were taken to assess the noise. Image size, 76.98 µm × 76.98 µm, was chosen to be able to monitor two neighboring cells to calculate the overall photobleaching and evaluate focal plane drifts during postbleaching data acquisition. The monitored fluorescence recovery plateau was between 100 and 150 s at 23°C with mobile fraction >80%. Sample rate was 120–280 images at a rate of 2.1 image/s. 20–25 cells (40–50 FRAP curves) of Orai1α Orai1β were obtained from 12 to 15 independent experiments. To compare recovery curves for different cells, we normalized the data to correct for variations in protein expression levels, background fluorescence, and loss of fluorescence during bleaching. The percentage of mobile fractions of the two Orai1 forms, background photobleaching correction, photofading factor, fit formula (mono exponential), fit range, and fit normalized recovery curve were calculated by the FRAP analysis module included in the ZenBlue 3.4 acquisition and analysis software from Zeiss (Fukushima et al., 2012).

## 2.6 | Statistical analysis

All data are presented as the mean ± standard error of mean (SEM). Analysis of statistical significance was performed using GraphPad Prism v.8.4.3 (GraphPad Software). Kruskal–Wallis test combined with Dunn's post hoc test were used to compare the different experimental groups. For comparison between two groups, the Mann–Whitney $U$ test was used. All data with $p < 0.05$ was deemed significant; "ns" = nonsignificant.

## 3 | RESULTS

### 3.1 | Translocation of Orai1 to the plasma membrane upon Ca²⁺-store depletion

Previous studies from our lab and others have demonstrated that there is a pool of compartmentalized Orai1 that translocates to the plasma membrane in response to $Ca^{2+}$-store discharge (Hodeify et al., 2018; Jardin et al., 2018; Woodard et al., 2008; Yu et al., 2010). By biotinylation of surface proteins, we have analyzed the role of TG, an inhibitor of the sarco/endoplasmic reticulum $Ca^{2+}$-ATPase (SERCA), on the plasma membrane expression of Orai1 using CRISPR/Cas9-generated Orai1-knockout (Orai1-KO) HEK-293 cells expressing wild-type (WT) Orai1, which is expected to yield a mixture of the two Orai1 variants. As shown in Figure 1a, plasma membrane expression of Orai1 was detected in resting cells, and stimulation with 2 μM TG significantly enhanced the amount of Orai1 resident in the plasma membrane ($n = 6$). Expression of functional Orai1 was confirmed by the determination of SOCE in these cells. Treatment of Orai1-KO HEK-293 cells expressing WT-Orai1, perfused with a $Ca^{2+}$-free medium, with 2 μM TG resulted in a transient increase in the fura-2 fluorescence ratio as a result of $Ca^{2+}$ release from the intracellular $Ca^{2+}$ stores. Subsequent addition of extracellular $Ca^{2+}$ leads to a rise in the fura-2 fluorescence ratio that is indicative of SOCE ($n = 10$–15 cells/day/4 days).

Chaperonin-containing T-complex protein 1 (CCT) has been reported to regulate Orai1 trafficking and residence in the plasma membrane in Chinese hamster ovary (CHO) cells by its interaction with the Orai1-CCT binding domain located in the intracellular loop between residues 157 and 167 (Hodeify et al., 2018). Hence, we have further explored whether this mechanism also regulates the plasma membrane expression of Orai1 in HEK-293 cells. Cells were transfected with expression plasmid of a mutant Orai1 bearing the scrambled sequence 157NEKPHRSLVES167 (Orai1 157-167sc), which prevents CCT-Orai1 interaction (Hodeify et al., 2018). As shown in Figure 1a, cells expressing the Orai1 157-167sc mutant exhibited a significantly greater expression of Orai1 in the plasma membrane at rest than cells expressing WT-Orai1 ($p < 0.05$; $n = 6$), which is consistent with the crucial role of CCT in Orai1 endocytosis reported by Hodeify and coworkers (Hodeify et al., 2018). Under these conditions, cell stimulation with TG did not significantly modify the amount of plasma membrane resident Orai1. In cells expressing the Orai1 157–167sc mutant, SOCE was significantly greater than in cells expressing WT-Orai1, which is consistent with the greater amount of Orai1 expressed in the plasma membrane (Figure 1b; $p < 0.05$; $n = 10$–15 cells/day/4 days).

### 3.2 | Plasma membrane location of Orai1α and Orai1β upon Ca²⁺-store depletion

Previous studies have provided evidence supporting that Orai1β is more efficient than Orai1α supporting SOCE in mouse embryonic fibroblasts (Desai et al., 2015). These findings are consistent with the lower sensitivity of Orai1β to $Ca^{2+}$-dependent inactivation demonstrated in HEK-293 cells (Desai et al., 2015). We have now explored the efficacy of Orai1α and Orai1β supporting SOCE in HEK-293 cells. For this study, Orai1-KO HEK-293 cells were used to have a clean background. To identify potential differences between both Orai1 variants Orai1-KO cells were transfected with expression plasmids for Orai1α, Orai1β or both using thymidine kinase (TK) promoter, which results in a considerably smaller expression level than plasmids incorporating a CMV promoter (X. Zhang et al., 2019). As shown in Figure 2a, treatment of wild-type HEK-293 cells, perfused with a $Ca^{2+}$-free medium, with 2 μM TG induced a transient increase in the fura-2 fluorescence ratio due to $Ca^{2+}$ release from the intracellular $Ca^{2+}$ stores. Subsequent addition of extracellular $Ca^{2+}$ results in a rise in the fura-2 fluorescence ratio indicative of SOCE. As expected, in Orai1-KO cells, TG-evoked $Ca^{2+}$ entry was essentially abrogated, and the expression of either Orai1α or Orai1β rescued SOCE in these cells (Figure 2a). Interestingly, we found that in Orai1-KO cells expressing Orai1α TG-induced SOCE was greater than in Orai1-KO cells expressing Orai1β, thus suggesting that the efficacy of Orai1α supporting SOCE in Orai1-KO HEK-293 cells was greater than that of Orai1β (Figure 2a); therefore, we analyzed the plasma membrane expression of both variants under these experimental conditions. Orai1-KO cells and Orai1-KO cells expressing either Orai1α, Orai1β or both variants were stimulated for 1 min in a medium containing 1.8 mM $Ca^{2+}$ with TG or left untreated, and the plasma membrane location of the Orai1 variants was analyzed by surface biotinylation. As shown in Figure 2b, Orai1α and Orai1β were detected in the plasma membrane in resting conditions when they were expressed alone or in combination. In Orai1-KO cells expressing Orai1α, $Ca^{2+}$ store depletion by TG significantly increased the plasma membrane expression of Orai1α by 36 ± 1% as compared to nonstimulated cells. By contrast, TG was unable to enhance the surface expression of Orai1β over the pretreatment level when expressed alone in Orai1-KO cells. Interestingly, in cells expressing both variants TG significantly enhanced over the pretreatment level the plasma membrane expression of Orai1α and Orai1β by 39 ± 8 and 81 ± 2%, respectively (Figure 2b), thus suggesting that agonist-induced plasma membrane location of the intracellular pool of Orai1β requires co-expression of Orai1α. These findings are consistent with the analysis of SOCE in Orai1-KO cells expressing both Orai1α and Orai1β, which was significantly greater than that observed in WT and Orai1-KO cells expressing either Orai1α or Orai1β alone (Figure 2a).

The plasma membrane expression of intracellularly located Orai1 variants upon stimulation with TG was further analyzed by fluorescence recovery after photobleaching (FRAP). FRAP measurements were carried out on an LSM900 confocal microscope as described in Section 2. As shown in Figure 2c, the recovery of both Orai1 variants in resting cells occurred efficiently in approximately 150 s and treatment with TG significantly enhanced the recovery of Orai1α but not Orai1β when expressed independently. These findings further confirm the expression of an additional pool of Orai1α in the plasma membrane upon $Ca^{2+}$ store depletion by TG, an event that is lacking in Orai1β in the absence of Orai1α. To confirm that agonist-induced further plasma membrane location of Orai1β requires co-expression of Orai1α, as detected by biotinylation, we co-expressed Orai1β-GFP with Orai1α-CFP and analyzed GFP FRAP. As shown in Figure S1, Orai1α-CFP exhibited a
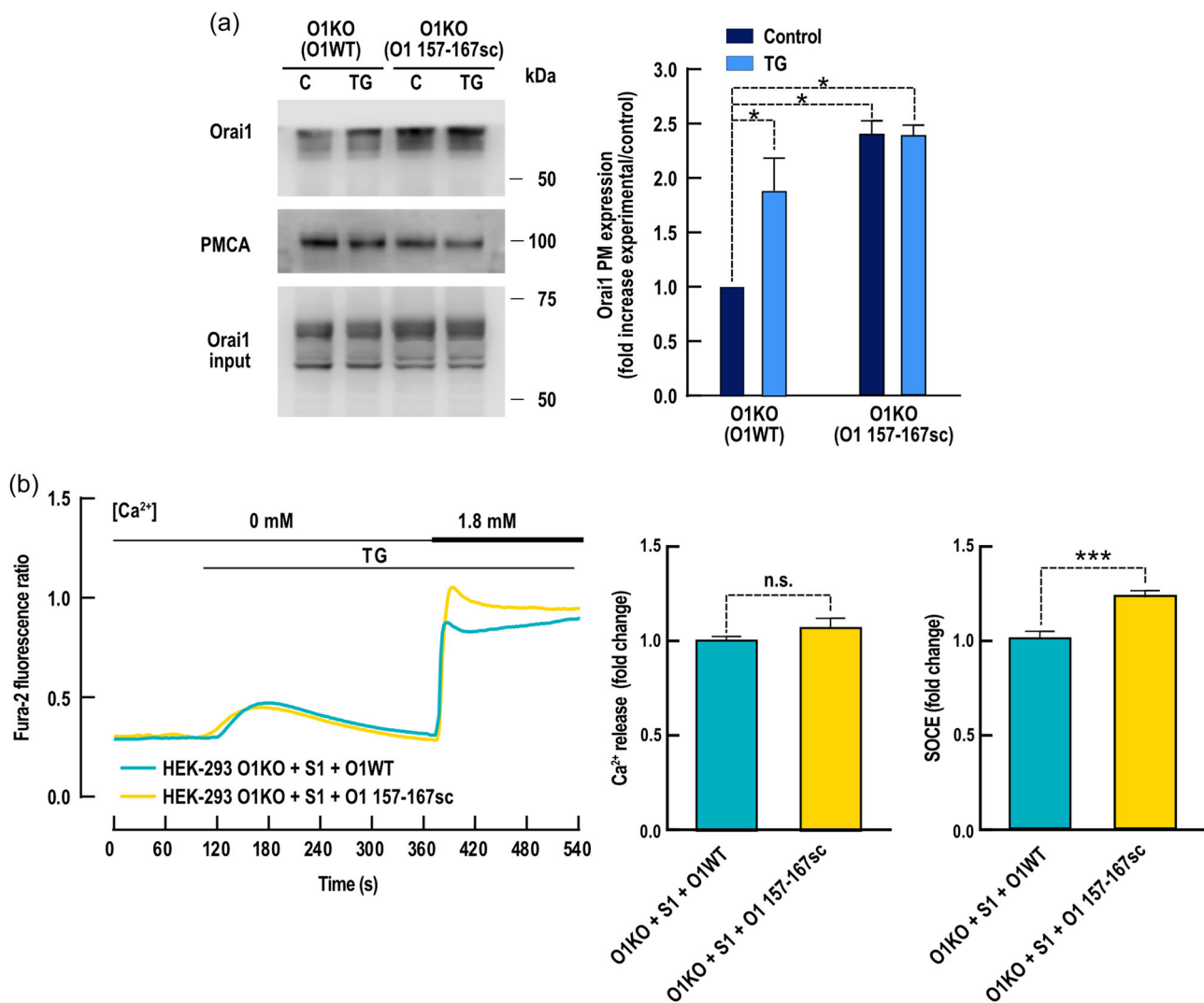
**FIGURE 1** Plasma membrane expression of an Orai1 mutant with residues 157 to 167 scrambled. (a) Orai1-KO HEK-293 cells expressing either Orai1 WT (O1KO(O1WT)) or an Orai1 construct with residues 157–167 scrambled (O1KO(O1 157–167sc)) were suspended in a medium containing 1.8 mM $CaCl_2$, and then stimulated with 2 μM TG or left untreated. Samples were then mixed with biotinylation buffer containing EZ-Link sulfo-NHS-LC-biotin, and cell surface proteins were labeled by biotinylation. Labeled proteins were pulled down with streptavidin-coated agarose beads. The pellet (containing the plasma membrane fraction) was analyzed by SDS-PAGE and western blot analysis using anti-Orai1 antibody, as indicated. Molecular masses indicated on the right were determined using molecular-mass markers run in the same gel. Membranes were probed with anti-PMCA antibody. These results are representative of six separate experiments. Quantification of Orai1 plasma membrane expression under the different experimental conditions normalized to the PMCA expression is depicted in the bar graph. Data are represented as mean ± SEM and were statistically analyzed using Kruskal–Wallis test with multiple comparisons (Dunn's test). *$p < 0.05$ as compared with control O1KO(O1WT) cells. (b) Representative $Ca^{2+}$ mobilization in response to 2 μM thapsigargin (TG) measured using fura-2 in Orai1-KO HEK-293 cells (HEK-293 O1KO) expressing STIM1 and either Orai1 WT (O1WT) or an Orai1 construct with residues 157 to 167 scrambled (O1KO (O1 157–167sc)), as described. Cells were superfused with a $Ca^{2+}$-free HBS (100 μM EGTA added) and stimulated with 2 μM TG, followed by re-addition of $CaCl_2$ (1.8 mM) to estimate $Ca^{2+}$ influx. Quantification of TG-evoked $Ca^{2+}$ release from the intracellular stores and entry is shown in the bar graphs. Traces are representative of 10–15 cells/day/4 days. Data are represented as mean ± SEM and were statistically analyzed using the Mann–Whitney $U$ test. ***$p < 0.001$ as compared with control. SDS-PAGE, sodium dodecyl sulfate-polyacrylamide gel electrophoresis SEM, standard error of mean; TG, thapsigargin; WT, wild-type.

similar plasma membrane distribution than Orai1β-GFP. Furthermore, while Orai1α-CFP was detected upon excitation at 405 nm, no CFP fluorescence was detected at 488 nm, thus suggesting that Orai1β-GFP detection is not contaminated by the expression of Orai1α-CFP (Figure S1). As shown in Figure 2c, in the presence of Orai1α, TG significantly enhanced the recovery of Orai1β, thus

suggesting that expression of an additional pool of Orai1β upon agonist stimulation requires the presence of Orai1α.Next, we explored the involvement of $Ca^{2+}$ mobilization in TG-induced translocation of Orai1 variants to the plasma membrane. To test the role of $Ca^{2+}$ influx in this process cells were perfused with a $Ca^{2+}$-free medium, and the plasma membrane location of Orai1α

and Orai1β was assessed by surface biotinylation as described above. As shown in Figure 3a, treatment with TG, in the absence of extracellular $Ca^{2+}$, significantly enhanced the plasma membrane location of Orai1α, but not Orai1β, when expressed individually, but in cells co-expressing both Orai1 forms TG increases the plasma membrane expression of Orai1α and Orai1β. The extent of plasma membrane expression of Orai1α and Orai1β detected in the absence of extracellular $Ca^{2+}$ was similar to that observed in
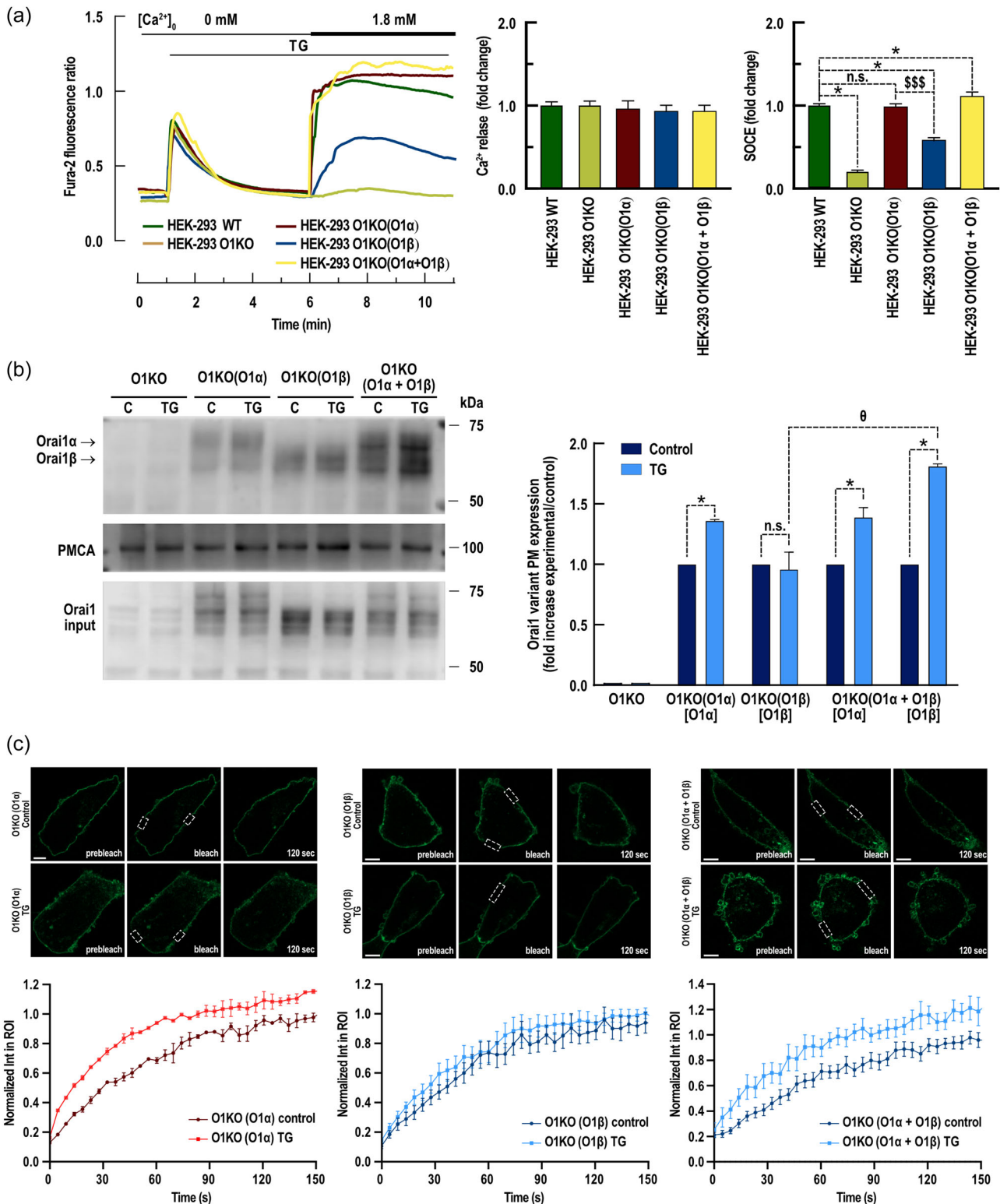


FIGURE 2 (See caption on next page)

the presence of 1.8 mM $Ca^{2+}$, thus indicating that $Ca^{2+}$ influx is not required for the translocation of compartmentalized Orai1 variants to the plasma membrane. To further analyzed the role of $Ca^{2+}$ mobilization from intracellular stores in the translocation of Orai1 variants to the plasma membrane, cells were loaded with the intracellular $Ca^{2+}$ chelator dimethyl BAPTA, by incubation with 10 µM dimethyl BAPTA/AM for 30 min as described in Methods, which prevents TG-evoked rises in $[Ca^{2+}]_c$ (data not shown). As shown in Figure 3b, dimethyl BAPTA loading did not significantly modified the pattern of plasma membrane expression of the Orai1 variants induced by TG, which strongly suggests that TG-evoked Orai1 variants trafficking and residence in the plasma membrane is independent on the rises in $[Ca^{2+}]_c$.

## 3.3 | Orai1α and Orai1β trafficking to the plasma membrane upon $Ca^{2+}$-store depletion is supported by the actin cytoskeleton

We have further investigated role of the actin cytoskeleton in TG-induced translocation of Orai1 variants to the plasma membrane. Orai1-KO cells and Orai1-KO cells expressing Orai1α alone or in combination with Orai1β were pretreated for 40 min with 10 µM cytochalasin D (Cyt D), a widely utilized membrane-permeant inhibitor of actin polymerization (Galan et al., 2011), or the vehicle, and then stimulated for 1 min in a medium containing 1.8 mM $Ca^{2+}$ in the absence or presence of TG and the plasma membrane location of the Orai1 variants was analyzed by surface biotinylation. As shown in Figure 4a, in cells pretreated with Cyt D TG was unable to induce

trafficking of Orai1α and Orai1β (when co-expressed with Orai1α) to the plasma membrane, which indicates that this process is supported by the actin cytoskeleton.

The role of the actin cytoskeleton in the plasma membrane expression of intracellularly located Orai1α upon stimulation with TG was further analyzed by fluorescence recovery after photobleaching (FRAP). Orai1-KO cells expressing either Orai1α-GFP, Orai1β-GFP or Orai1α-CFP and Orai1β-GFP were pretreated with Cyt D 40 min before the stimulation with TG. As shown in Figure 4b, the recovery of both Orai1 variants in resting cells occurred efficiently in cells pretreated with Cyt D or the vehicle, but the additional recovery of Orai1α evoked by TG was abolished upon inhibition of actin filament polymerization (Figure 4b, left panel). As shown above, TG was unable to enhance the recovery of Orai1β when expressed alone (Figure 4b, middle panel) but, when co-expressed with Orai1α, TG significantly enhanced the recovery of Orai1β, an effect that was abrogated by pretreament with Cyt D (Figure 4b, right panel). These findings indicate that the trafficking and plasma membrane location of Orai1 variants induced by TG was strongly dependent on actin filament reorganization.

## 3.4 | Orai1α and Orai1β trafficking to the plasma membrane upon $Ca^{2+}$-store depletion requires functional ARF6

ARF6 regulates endosomal plasma membrane trafficking in many cell types (Aikawa & Martin, 2003). ARF6 has been reported to mediate constitutive recycling of Orai1 in _Xenopus_ oocytes and HEK-293 cells

**FIGURE 2** Distribution of Orai1α and Orai1β in the plasma membrane at rest and upon stimulation with thapsigargin. (a) Representative $Ca^{2+}$ mobilization in response to 2 µM thapsigargin (TG) measured using fura-2 in wild-type HEK-293 cells (HEK-293 WT), Orai1-KO HEK-293 cells (HEK-293 O1KO) and Orai1-KO HEK-293 cells expressing either Orai1α (HEK-293O1KO(O1α)), Orai1β (HEK-293O1KO(O1β)) or both (HEK-293O1KO(O1α + O1β)), as described. Cells were superfused with a $Ca^{2+}$-free HBS (100 µM EGTA added) and stimulated with 2 µM TG followed by re-addition of $CaCl_2$ (1.8 mM) to estimate $Ca^{2+}$ influx. Quantification of TG-evoked $Ca^{2+}$ release from the intracellular stores and entry is shown in the bar graphs. Traces are representative of 10–15 cells/day/4 days. Data are represented as mean ± SEM and were statistically analyzed using Kruskal–Wallis test with multiple comparisons (Dunn's test). *$p < 0.05$ and $^{\$\$\$}p < 0.001$. (b) Orai1-KO HEK-293 cells (O1KO), and Orai1-KO HEK-293 cells expressing either Orai1α (O1KO(O1α)), Orai1β (O1KO(O1β)) or both (O1KO(O1α + O1β)) were suspended in a medium containing 1.8 mM $CaCl_2$, and then stimulated for 1 min with 2 µM TG or left untreated. Samples were then mixed with biotinylation buffer containing EZ-Link sulfo-NHS-LC-biotin, and cell surface proteins were labeled by biotinylation. Labeled proteins were pulled down with streptavidin-coated agarose beads. The pellet (containing the plasma membrane fraction) and the supernatant were analyzed by SDS-PAGE and western blot analysis using anti-Orai1 antibody, as indicated (top (pellet) and bottom (supernatant) panels). Membranes were probed with anti-PMCA antibody. Molecular masses indicated on the right were determined using molecular-mass markers run in the same gel. These results are representative of 6 separate experiments. Quantification of Orai1 plasma membrane expression under the different experimental conditions normalized to the PMCA expression is depicted in the bar graph. Data are represented as mean ± SEM and were statistically analyzed using Kruskal–Wallis test with multiple comparisons (Dunn's test). *$p < 0.05$ as compared with their respective control. $^{\varphi}p < 0.05$ as compared with TG-stimulated O1KO(O1β) cells. (c) HEK-293 O1KO cells expressing either Orai1α-GFP (O1KO(O1α)), Orai1β-GFP (O1KO(O1β)) or Orai1α-CFP and Orai1β-GFP (O1KO(O1α + O1β)) were mounted on an inverted LSM900 confocal microscope (Carl Zeiss). Cells were suspended in a medium containing 1.8 mM $CaCl_2$, and then stimulated with 2 µM TG or left untreated, as indicated. The mobility of Orai1α (left panel) or Orai1β (middle and right panels) was determined by using fluorescence recovery after photobleaching (FRAP) as described in Section 2. The graphs represent the fit normalized recovery curves of both Orai1 variants in resting and upon stimulation. SDS-PAGE, sodium dodecyl sulfate-polyacrylamide gel electrophoresis SEM, standard error of mean; WT, wild-type.
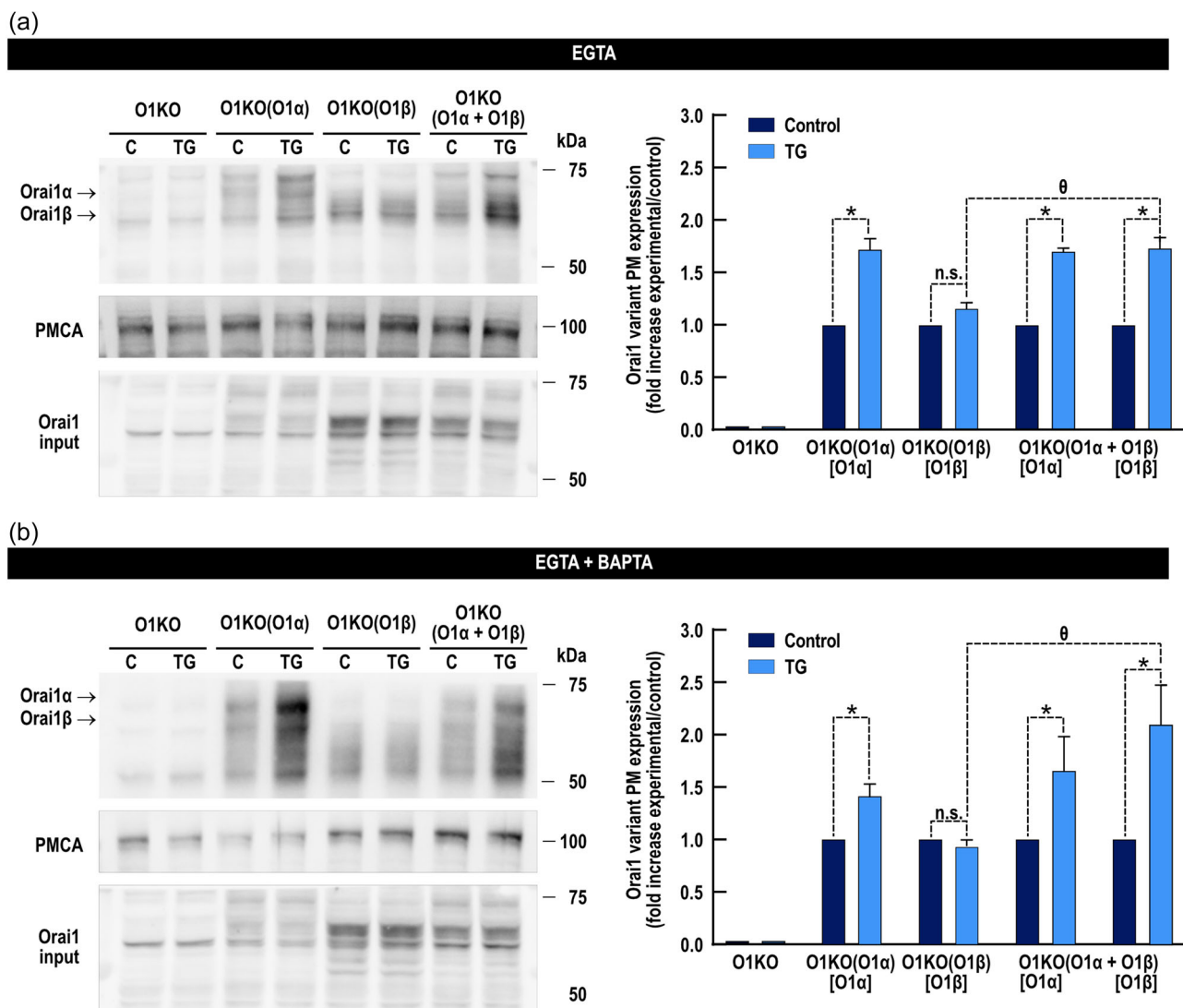
—WILEY—

**FIGURE 3** Role of intracellular $Ca^{2+}$ in the plasma membrane location of Orai1α and Orai1β at rest and upon stimulation with thapsigargin. Orai1-KO HEK-293 cells (O1KO), and Orai1-KO HEK-293 cells expressing either Orai1α (O1KO(O1α)), Orai1β (O1KO(O1β)) or both (O1KO (O1α + O1β)) were either loaded with dimethyl BAPTA (b) or treated with vehicle (a) and suspended in a $Ca^{2+}$-free medium (100 μM EGTA added). Cells were then stimulated for 1 min with 2 μM TG or left untreated. Samples were then mixed with biotinylation buffer containing EZ-Link sulfo-NHS-LC-biotin, and cell surface proteins were labeled by biotinylation. Labeled proteins were pulled down with streptavidin-coated agarose beads. The pellet (containing the plasma membrane fraction) and the supernatant were analyzed by SDS-PAGE and western blot analysis using anti-Orai1 antibody, as indicated (top (pellet) and bottom (supernatant) panels). Membranes were probed with anti-PMCA antibody. Molecular masses indicated on the right were determined using molecular-mass markers run in the same gel. These results are representative of six separate experiments. Quantification of Orai1 plasma membrane expression under the different experimental conditions normalized to the PMCA expression is depicted in the bar graph. Data are represented as mean ± SEM and were statistically analyzed using Kruskal–Wallis test with multiple comparisons (Dunn's test). *$p < 0.05$ as compared with their respective control. $^{φ}p < 0.05$ as compared with TG-stimulated O1KO(O1β) cells. SDS-PAGE, sodium dodecyl sulfate-polyacrylamide gel electrophoresis SEM, standard error of mean; TG, thapsigargin; WT, wild-type.

(Yeh et al., 2020; Yu et al., 2010). We have investigated the involvement of ARF6 in TG-induced trafficking of Orai1 variants to the plasma membrane by overexpressing either wild-type ARF6 (ARF6wt) or a dominant negative ARF6 mutant (ARF6-T27N; ARF6dn). Orai1-KO cells expressing Orai1α alone or in combination with Orai1β were transfected with expression plasmids for ARF6wt or ARF6dn or empty vector. Forty-eight hours after transfection cells were stimulated for 1 min in a medium containing 1.8 mM $Ca^{2+}$ in the absence or presence of TG and the plasma membrane location of the Orai1 variants was analyzed by surface biotinylation. As shown in Figure 5a, in cells expressing ARF6wt TG-induced translocation of Orai1α and Orai1β (when co-expressed with Orai1α) to the plasma membrane was not significantly modified; however, expression of ARF6dn essentially abolished TG-evoked trafficking of Orai1α and Orai1β to the plasma membrane, which indicates that this process requires functional ARF6.
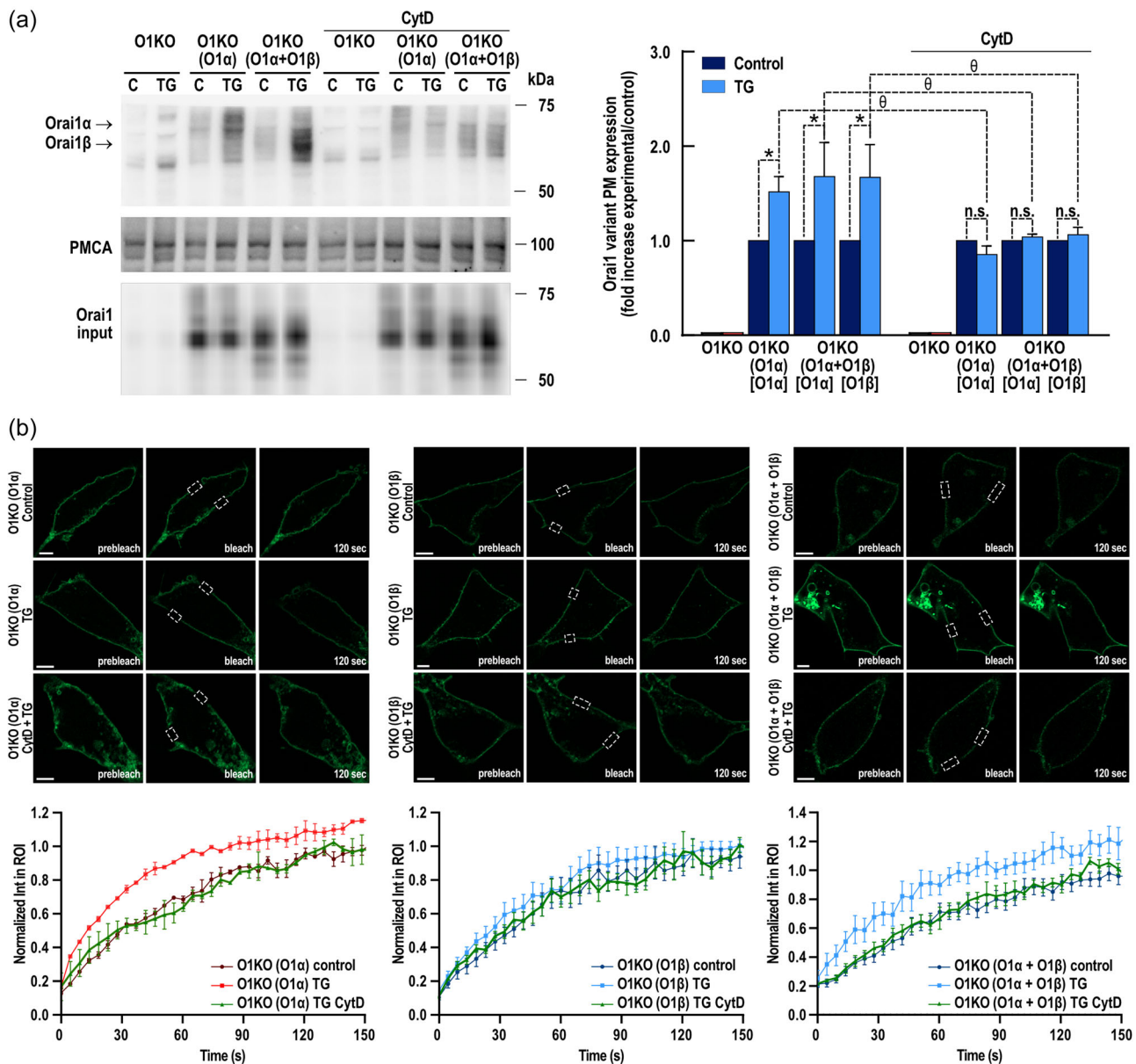
(a)



(b)



**FIGURE 4** Effect of cytochalasin D on the plasma membrane location of Orai1α and Orai1β at rest and thapsigargin-treated cells. (a) Orai1-KO HEK-293 cells (O1KO), and Orai1-KO HEK-293 cells expressing either Orai1α (O1KO(O1α)), Orai1β (O1KO(O1β)) or both (O1KO (O1α + O1β)) were pretreated with 10 μM cytochalasin D or the vehicle for 40 min, as indicated. Cells were suspended in a medium containing 1.8 mM CaCl$_2$, and then stimulated for 1 min with 2 μM TG or left untreated. Samples were then mixed with biotinylation buffer containing EZ-Link sulfo-NHS-LC-biotin, and cell surface proteins were labeled by biotinylation. Labeled proteins were pulled down with streptavidin-coated agarose beads. The pellet (containing the plasma membrane fraction) and the supernatant were analyzed by SDS-PAGE and western blot analysis using anti-Orai1 antibody, as indicated (top (pellet) and bottom (supernatant) panels). Membranes were probed with anti-PMCA antibody. Molecular masses indicated on the right were determined using molecular-mass markers run in the same gel. These results are representative of six separate experiments. Quantification of Orai1 plasma membrane expression under the different experimental conditions normalized to the PMCA expression is depicted in the bar graph. Data are represented as mean ± SEM and were statistically analyzed using Kruskal–Wallis test with multiple comparisons (Dunn's test). *$p < 0.05$ as compared with their respective control. $^\varphi p < 0.05$ as compared with the corresponding TG-stimulated cells not pretreated with cytochalasin D. (b) HEK-293 O1KO expressing either Orai1α (O1KO(O1α)), Orai1β (O1KO(O1β)) or Orai1α-CFP and Orai1β-GFP (O1KO(O1α + O1β)) were pretreated with 10 μM cytochalasin D or the vehicle for 40 min, as indicated, and mounted on an inverted LSM900 confocal microscope (Carl Zeiss). Cells were suspended in a medium containing 1.8 mM CaCl$_2$, and then stimulated with 2 μM TG, or left untreated. The mobility of Orai1α (left panel) or Orai1β (middle and right panels) was determined by using fluorescence recovery after photobleaching (FRAP) as described in Section 2. The graphs represent the fit normalized recovery curves of both Orai1 variants in resting and upon stimulation.
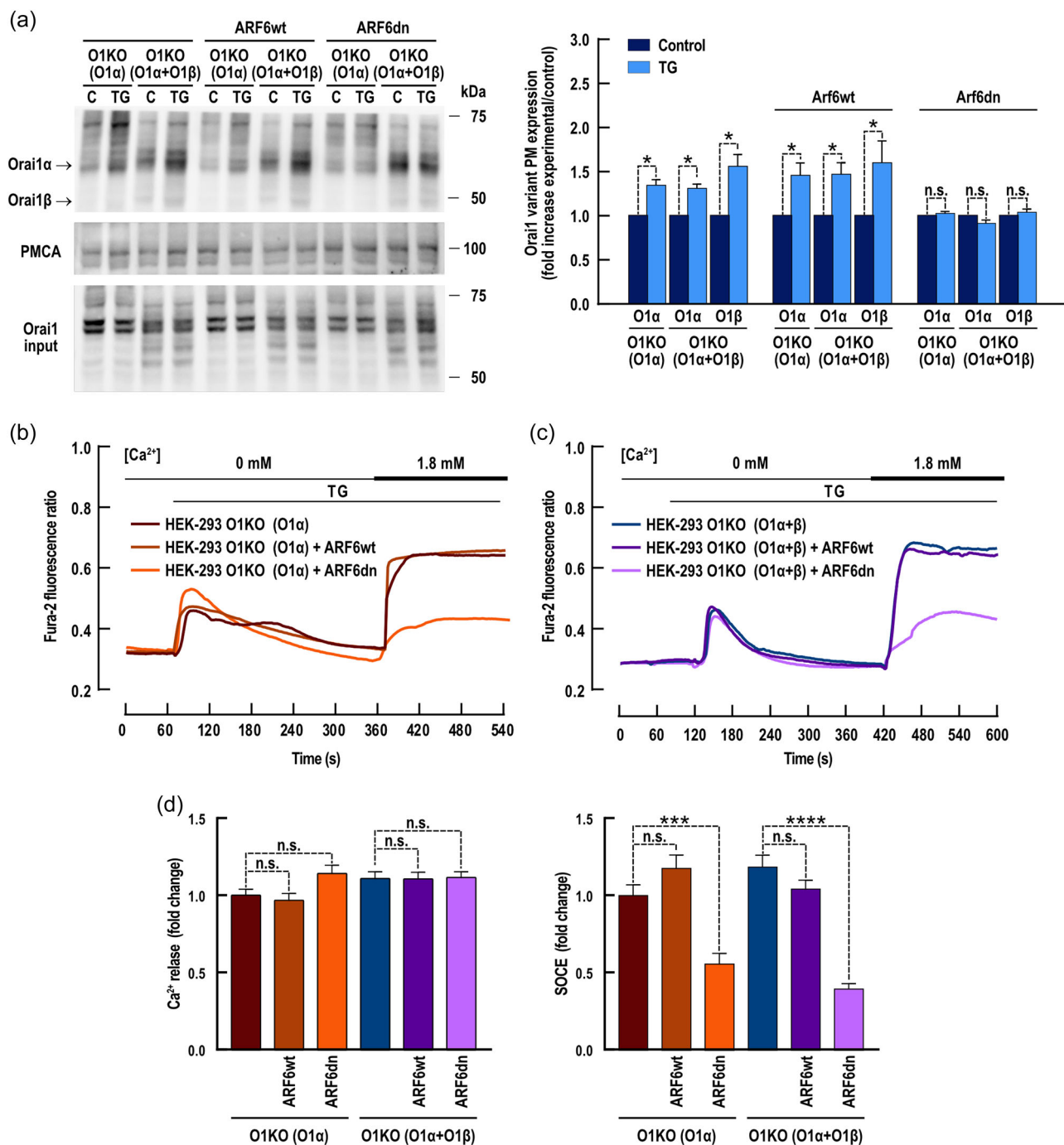
**FIGURE 5** Role of ARF6 in the plasma membrane expression of an Orai1 upon stimulation with thapsigargin. (a) Orai1-KO HEK-293 cells expressing either Orai1α (O1KO(O1α)) or Orai1α and Orai1β (O1KO(O1α + O1β)) were transfected with expression plasmid for wild-type ARF6 (ARF6wt), a dominant negative mutant of ARF6 (ARF6dn) or empty vector. Forty-eight hours later cells were suspended in a medium containing 1.8 mM CaCl$_2$, and then stimulated for 1 min with 2 μM TG or left untreated. Samples were then mixed with biotinylation buffer containing EZ-Link sulfo-NHS-LC-biotin, and cell surface proteins were labeled by biotinylation. Labeled proteins were pulled down with streptavidin-coated agarose beads. The pellet (containing the plasma membrane fraction) and the supernatant were analyzed by SDS-PAGE and western blot analysis using anti-Orai1 antibody, as indicated (top (pellet) and bottom (supernatant) panels). Membranes were probed with anti-PMCA antibody. Molecular masses indicated on the right were determined using molecular-mass markers run in the same gel. Membranes were probed with anti-PMCA antibody. These results are representative of six separate experiments. Quantification of Orai1 plasma membrane expression under the different experimental conditions normalized to the PMCA expression is depicted in the bar graph. Data are represented as mean ± SEM and were statistically analyzed using Kruskal–Wallis test with multiple comparisons (Dunn's test). *p < 0.05. (b and c) Representative Ca$^{2+}$ mobilization in response to 2 μM thapsigargin (TG) measured using fura-2 in Orai1-KO HEK-293 cells expressing Orai1α or Orai1α and Orai1β alone or in combination with wild-type ARF6 (ARF6wt) or a dominant negative mutant of ARF6 (ARF6dn), as described. Cells were superfused with a Ca$^{2+}$-free HBS (100 μM EGTA added) and stimulated with 2 μM TG, followed by re-addition of CaCl$_2$ (1.8 mM) to estimate Ca$^{2+}$ influx. (d) Quantification of TG-evoked Ca$^{2+}$ release from the intracellular stores and entry is shown in the bar graphs. Data are represented as mean ± SEM and were statistically analyzed using Kruskal–Wallis test with multiple comparisons (Dunn's test). ***p < 0.001 and ****p < 0.0001. SDS-PAGE, sodium dodecyl sulfate-polyacrylamide gel electrophoresis SEM, standard error of mean; WT, wild-type.

Analysis of TG-stimulated $Ca^{2+}$ mobilization in Orai1-KO cells expressing Orai1α alone or in combination with Orai1β revealed that expression of ARF6wt did not significantly alter either TG-induced $Ca^{2+}$ release or entry; however, in cells expressing ARF6dn, TG-evoked SOCE was significantly attenuated, without having any effect on $Ca^{2+}$ release from the intracellular stores (Figure 5b). These findings further confirm the functional role of ARF6 in TG-induced trafficking of Orai1 variants to the plasma membrane and supports an important role for this mechanism in TG-evoked SOCE.

# 4 | DISCUSSION

Orai1α and Orai1β were identified in 2012 as two Orai1 variants generated by alternative translation initiation from the same transcript (Fukushima et al., 2012). Both Orai1 forms have been reported to support $I_{CRAC}$ with similar efficiency (Desai et al., 2015). However, the participation of both variants in $I_{SOC}$ has been reported to be cell specific (Sanchez-Collado et al., 2022), and only Orai1α is involved in the arachidonate-regulated $Ca^{2+}$ current $I_{ARC}$ (Desai et al., 2015). The 63 amino acids located in the N-terminal region of Orai1α mediates the association of this variant with a number of interacting partners, such as caveolin, that might lead to different plasma membrane location and mobilities between the two Orai1 forms. As a result, Orai1α and Orai1β have been shown to exhibit distinct plasma membrane mobilities in resting cells as detected by FRAP, where Orai1β shows a faster diffusion than the majority of Orai1α subunits (Fukushima et al., 2012). These, and other observations (Desai et al., 2015; Sanchez-Collado et al., 2022), suggest that both Orai1 variants do not form hetero-multimeric channels or, at least, that is not the predominant presentation. Here, we show that Orai1α and Orai1β exhibit differences in the trafficking and plasma membrane expression upon $Ca^{2+}$ store depletion. It has been reported that, in addition to the plasma membrane pool of Orai1, there is a subset of Orai1 located in an endosomal compartment that is inserted in the plasma membrane upon $Ca^{2+}$ store depletion in an exocytotic manner that involves proteins such as SNAP25 (synaptosomal-associated protein-25) and Rho (Woodard et al., 2008; Yu et al., 2010). Our results indicate that when Orai1α and Orai1β are expressed either singly or together in Orai1-KO HEK-293 cells a subset of the proteins is constitutively expressed in the plasma membrane. When the Orai1 variants are individually expressed, store depletion induces a significant increase in the plasma membrane expression of Orai1α, while the expression of the compartmentalized Orai1β requires the presence of Orai1α. These findings suggest that there is some form of functional interaction between both variants, so the trafficking of both Orai1 forms is associated with Orai1α, but this is unknown at present.

Store depletion-associated trafficking of compartmentalized Orai1 variants is independent of $Ca^{2+}$ influx and intracellular $Ca^{2+}$ mobilization and, according to the FRAP analysis, occurs within the first few seconds after store depletion. Furthermore, this mechanism is strongly dependent on the integrity of the actin filament network, which suggests that the actin cytoskeleton supports the translocation

of the Orai1 forms to the plasma membrane. This observation is consistent with the regulation of plasma membrane abundance of other $Ca^{2+}$ channels, such as $Ca_v1.2$ by exocytic and post-endocytic trafficking to the cell surface (Conrad et al., 2018).

Orai1 recycling at the plasma membrane has been reported to involve the CCT chaperonin complex, required for Orai1 endocytosis (Hodeify et al., 2018), as well as a constitutive exocytosis with a rate constant of approximately $0.1\,min^{-1}$ (Hodeify et al., 2015). Furthermore, Orai1 plasma membrane abundance is enhanced by different mechanisms, including $Ca^{2+}$ store depletion (Woodard et al., 2008) or the secretory pathway $Ca^{2+}$-ATPase (SPCA) in specialized mammary epithelial cells associated to store-independent $Ca^{2+}$ entry (Cross et al., 2013). Concerning the trafficking of Orai1 to the plasma membrane upon store depletion, we previously reported that the mechanism involves the participation of SNAP-25 (Woodard et al., 2008), and here, we present evidence for the involvement of the adenosine diphosphate ribosylation factor ARF6, as expression of the dominant negative ARF6-T27N mutant abolished store depletion-evoked translocation of Orai1 to the plasma membrane. We noticed that while expression of the dominant negative ARF6 mutant attenuated Orai1 variants expression in the plasma membrane and SOCE, expression of WT-ARF6 did not significantly enhance these processes. We attribute this observation to the fact that ARF6 is necessary for the translocation of Orai1 to the plasma membrane, but the native expression of ARF6 might be sufficient to support this mechanism, so that overexpression of the protein does not have an increasing effect on Orai1 expression at the plasma membrane. ARF6 has been reported to participate in internalization of TRPC1 during the recycling of this channel (de Souza et al., 2015). Furthermore, ARF6 modulates SOCE, as a downstream effector of RAS association domain family 4 (RASSF4), by regulating the plasma membrane $PI(4,5)P_2$ levels (Chen et al., 2017). More recently, in patients with atopic dermatitis, ARF6 has been shown to mediate the exocytic insertion of the Orai1 single-nucleotide polymorphisms S218G–Orai1 and N223S–Orai1 in the plasma membrane, thus escaping from degradation, which leads to a mismatch in the Orai1–STIM stoichiometry and, consequently, to attenuation of SOCE and the associated gene expression (Yeh et al., 2020).

Summarizing, our results indicate that $Ca^{2+}$ store depletion modulates the cell surface abundance of Orai1α and Orai1β by a mechanism dependent on ARF6 and the actin filament network but independent on intracellular $Ca^{2+}$ mobilization. Interestingly, while Orai1β constitutively translocates to the plasma membrane in resting cells with a similar efficiency as Orai1α, the former acts as a defective form that requires the presence of Orai1α for the trafficking of compartmentalized subunits to the plasma membrane upon store depletion. Current evidence indicates that the Orai1α/Orai1β expression ratio ranges from 0.3 in nontumoral breast epithelial MCF10A cells to slightly over 1 in Jurkat cells (Fukushima et al., 2012; Sanchez-Collado et al., 2019) due to still unknown mechanism. In this context, the mechanism reported here might facilitate that cells express both variants evenly on the cell surface independently on the Orai1α/Orai1β expression ratio.

## AUTHOR CONTRIBUTIONS

Juan A. Rosado, Isaac Jardin, and Gines M. Salido: Conceptualization. Sandra Alvarado, Isaac Jardin, Jose Sanchez-Collado, and Jose J. Lopez: Methodology. Sandra Alvarado, Isaac Jardin, Jose J. Lopez, Joel Nieto-Felipe, Jose Sanchez-Collado: Investigation. Juan A. Rosado and Isaac Jardin: Validation. Juan A. Rosado and Gines M. Salido: Supervision. Juan A. Rosado: Writing-original draft. Isaac Jardin, Gines M. Salido, Jose J. Lopez, Joel Nieto-Felipe, and Jose Sanchez-Collado: Writing-review & editing. Juan A. Rosado: Funding acquisition. Juan A. Rosado: Project administration.

## ACKNOWLEDGMENTS

## CONFLICT OF INTEREST STATEMENT

The authors declare no conflict of interest.

## ETHICS STATEMENT

Experimental procedures were approved by the local ethical committee (University of Extremadura).

## CONSENT FOR PUBLICATION

All authors have agreed to publish this manuscript in Journal of Cellular Physiology.

## ORCID

Isaac Jardin http://orcid.org/0000-0003-4575-8264
Jose Sanchez-Collado https://orcid.org/0000-0001-7602-9975
Joel Nieto-Felipe http://orcid.org/0000-0001-6342-3893
Jose J. Lopez https://orcid.org/0000-0002-5234-1478
Gines M. Salido https://orcid.org/0000-0002-8687-2445
Juan A. Rosado http://orcid.org/0000-0002-9749-2325

## REFERENCES

Ahmad, M., Narayanasamy, S., Ong, H. L., & Ambudkar, I. (2022). STIM proteins and regulation of SOCE in ER-PM junctions. *Biomolecules*, *12*(8), 1152. https://doi.org/10.3390/biom12081152

Aikawa, Y., & Martin, T. F. J. (2003). ARF6 regulates a plasma membrane pool of phosphatidylinositol(4,5)bisphosphate required for regulated exocytosis. *Journal of Cell Biology*, *162*(4), 647–659. https://doi.org/10.1083/jcb.200212142

Chen, Y. J., Chang, C. L., Lee, W. R., & Liou, J. (2017). RASSF4 controls SOCE and ER-PM junctions through regulation of PI(4,5)P(2). *Journal of Cell Biology*, *216*(7), 2011–2025. https://doi.org/10.1083/jcb.201606047

Cheng, K. T., Liu, X., Ong, H. L., Swaim, W., & Ambudkar, I. S. (2011). Local Ca²⁺ entry via Orai1 regulates plasma membrane recruitment of TRPC1 and controls cytosolic Ca²⁺ signals required for specific cell functions. *PLoS Biology*, *9*(3), e1001025. https://doi.org/10.1371/journal.pbio.1001025

Conrad, R., Stölting, G., Hendriks, J., Ruello, G., Kortzak, D., Jordan, N., Gensch, T., & Hidalgo, P. (2018). Rapid turnover of the cardiac L-type Ca(V)1.2 channel by endocytic recycling regulates its cell surface availability. *iScience*, *7*, 1–15. https://doi.org/10.1016/j.isci.2018.08.012

Cross, B. M., Hack, A., Reinhardt, T. A., & Rao, R. (2013). SPCA2 regulates Orai1 trafficking and store independent Ca²⁺ entry in a model of lactation. *PLoS One*, *8*(6), e67348. https://doi.org/10.1371/journal.pone.0067348

Desai, P. N., Zhang, X., Wu, S., Janoshazi, A., Bolimuntha, S., Putney, J. W., & Trebak, M. (2015). Multiple types of calcium channels arising from alternative translation initiation of the Orai1 message. *Science Signaling*, *8*(387), ra74. https://doi.org/10.1126/scisignal.aaa8323

de Souza, L. B., Ong, H. L., Liu, X., & Ambudkar, I. S. (2015). Fast endocytic recycling determines TRPC1-STIM1 clustering in ER-PM junctions and plasma membrane function of the channel. *Biochimica et Biophysica Acta (BBA) - Molecular Cell Research*, *1853*(10 Pt A), 2709–2721. https://doi.org/10.1016/j.bbamcr.2015.07.019

Emrich, S. M., Yoast, R. E., & Trebak, M. (2022). Physiological functions of CRAC channels. *Annual Review of Physiology*, *84*, 355–379. https://doi.org/10.1146/annurev-physiol-052521-013426

Emrich, S. M., Yoast, R. E., Xin, P., Arige, V., Wagner, L. E., Hempel, N., Gill, D. L., Sneyd, J., Yule, D. I., & Trebak, M. (2021). Omnitemporal choreographies of all five STIM/Orai and IP3Rs underlie the complexity of mammalian Ca²⁺ signaling. *Cell Reports*, *34*(9), 108760. https://doi.org/10.1016/j.celrep.2021.108760

Fukushima, M., Tomita, T., Janoshazi, A., & Putney, J. W. (2012). Alternative translation initiation gives rise to two isoforms of Orai1 with distinct plasma membrane mobilities. *Journal of Cell Science*, *125*(Pt 18), 4354–4361. https://doi.org/10.1242/jcs.104919

Galán, C., Dionisio, N., Smani, T., Salido, G. M., & Rosado, J. A. (2011). The cytoskeleton plays a modulatory role in the association between STIM1 and the Ca²⁺ channel subunits Orai1 and TRPC1. *Biochemical Pharmacology*, *82*(4), 400–410. https://doi.org/10.1016/j.bcp.2011.05.017

Hodeify, R., Nandakumar, M., Own, M., Courjaret, R. J., Graumann, J., Hubrack, S. Z., & Machaca, K. (2018). The CCT chaperonin is a novel regulator of Ca²⁺ signaling through modulation of Orai1 trafficking. *Science Advances*, *4*(9), eaau1935. https://doi.org/10.1126/sciadv.aau1935

Hodeify, R., Selvaraj, S., Wen, J., Arredouani, A., Hubrack, S., Dib, M., Al-Thani, S. N., McGraw, T., & Machaca, K. (2015). A STIM1-dependent 'trafficking trap' mechanism regulates Orai1 plasma membrane residence and Ca²⁺ influx levels. *Journal of Cell Science*, *128*(16), 3143–3154. https://doi.org/10.1242/jcs.172320

Jardin, I., Diez-Bello, R., Lopez, J., Redondo, P., Salido, G., Smani, T., & Rosado, J. (2018). TRPC6 channels are required for proliferation, migration and invasion of breast cancer cell lines by modulation of Orai1 and Orai3 surface exposure. *Cancers*, *10*(9), 331. https://doi.org/10.3390/cancers10090331

Jardin, I., Lopez, J. J., Salido, G. M., & Rosado, J. A. (2008). Orai1 mediates the interaction between STIM1 and hTRPC1 and regulates the mode of activation of hTRPC1-forming Ca²⁺ channels. *Journal of Biological Chemistry*, *283*(37), 25296–25304. https://doi.org/10.1074/jbc.M802904200

Kim, M. S., Zeng, W., Yuan, J. P., Shin, D. M., Worley, P. F., & Muallem, S. (2009). Native store-operated Ca²⁺ influx requires the channel function of Orai1 and TRPC1. *Journal of Biological Chemistry*, *284*(15), 9733–9741. https://doi.org/10.1074/jbc.M808097200

Lunz, V., Romanin, C., & Frischauf, I. (2019). STIM1 activation of Orai1. *Cell Calcium*, *77*, 29–38. https://doi.org/10.1016/j.ceca.2018.11.009

Nieto-Felipe, J., Sanchez-Collado, J., Jardin, I., Salido, G. M., Lopez, J. J., & Rosado, J. A. (2023). The store-operated Ca2+ channel Orai1α is required for agonist-evoked NF-κB activation by a mechanism dependent on PKCβ2. *Journal of Biological Chemistry*, *299*(2), 102882. https://doi.org/10.1016/j.jbc.2023.102882

Sanchez-Collado, J., Lopez, J. J., Jardin, I., Berna-Erro, A., Camello, P. J., Cantonero, C., Smani, T., Salido, G. M., & Rosado, J. A. (2022). Orai1α, but not Orai1β, co-localizes with TRPC1 and is required for its plasma membrane location and activation in HeLa cells. *Cellular and Molecular Life Sciences*, *79*(1), 33. https://doi.org/10.1007/s00018-021-04098-w

Sanchez-Collado, J., Lopez, J. J., Jardin, I., Camello, P. J., Falcon, D., Regodon, S., Salido, G. M., Smani, T., & Rosado, J. A. (2019). Adenylyl cyclase type 8 overexpression impairs phosphorylation-dependent Orai1 inactivation and promotes migration in MDA-MB-231 breast cancer cells. *Cancers*, *11*(11), 1624. https://doi.org/10.3390/cancers11111624

Woodard, G. E., Salido, G. M., & Rosado, J. A. (2008). Enhanced exocytotic-like insertion of Orai1 into the plasma membrane upon intracellular $Ca^{2+}$ store depletion. *American Journal of Physiology-Cell Physiology*, *294*(6), C1323–C1331.

Yeh, Y. C., Lin, Y. P., Kramer, H., & Parekh, A. B. (2020). Single-nucleotide polymorphisms in Orai1 associated with atopic dermatitis inhibit protein turnover, decrease calcium entry and disrupt calcium-dependent gene expression. *Human Molecular Genetics*, *29*(11), 1808–1823. https://doi.org/10.1093/hmg/ddz223

Yen, M., & Lewis, R. S. (2019). Numbers count: How STIM and Orai stoichiometry affect store-operated calcium entry. *Cell Calcium*, *79*, 35–43. https://doi.org/10.1016/j.ceca.2019.02.002

Yoast, R. E., Emrich, S. M., Zhang, X., Xin, P., Johnson, M. T., Fike, A. J., Walter, V., Hempel, N., Yule, D. I., Sneyd, J., Gill, D. L., & Trebak, M. (2020). The native ORAI channel trio underlies the diversity of $Ca^{2+}$ signaling events. *Nature Communications*, *11*(1), 2444. https://doi.org/10.1038/s41467-020-16232-6

Yu, F., Sun, L., & Machaca, K. (2010). Constitutive recycling of the store-operated $Ca^{2+}$ channel Orai1 and its internalization during meiosis. *Journal of Cell Biology*, *191*(3), 523–535. https://doi.org/10.1083/jcb.201006022

Zhang, X., Pathak, T., Yoast, R., Emrich, S., Xin, P., Nwokonko, R. M., Johnson, M., Wu, S., Delierneux, C., Gueguinou, M., Hempel, N., Putney, J. W., Gill, D. L., & Trebak, M. (2019). A calcium/cAMP signaling loop at the ORAI1 mouth drives channel inactivation to shape NFAT induction. *Nature Communications*, *10*(1), 1971. https://doi.org/10.1038/s41467-019-09593-0

Zhou, Y., Cai, X., Nwokonko, R. M., Loktionova, N. A., Wang, Y., & Gill, D. L. (2017). The STIM-Orai coupling interface and gating of the Orai1 channel. *Cell Calcium*, *63*, 8–13. https://doi.org/10.1016/j.ceca.2017.01.001

## SUPPORTING INFORMATION

Additional supporting information can be found online in the Supporting Information section at the end of this article.